Cyclical "Flipping" of Morphology in Block Copolymer Thin Films

Parvaneh Mokarian-Tabari,[†,‡,*] Timothy W. Collins,[†] Justin D. Holmes,[†,‡] and Michael A. Morris[†,‡]

[†]Materials Research Group, School of Chemistry and the Tyndall National Institute, University College Cork, Cork, Ireland, and
[‡]Centre for Research on Adaptive Nanostructures and Nanodevices (CRANN), Trinity College Dublin, Dublin, Ireland

ABSTRACT We studied the kinetics of nanopattern evolution in (polystyrene-*b*-polyethylene oxide) diblock copolymer thin films. Using scanning force microscopy, a highly unexpected cylindrical flipping of morphology from normal to parallel to the film plane was detected during solvent annealing of the film (with average thickness of 30 nm) at high vapor pressure. Using an *in situ* time-resolved light scattering device combined with an environmental cell enabled us to obtain kinetic information at different vapor pressures. The data indicated that there is a threshold value for the vapor pressure necessary for the structural transition. We propose a swelling and deswelling mechanism for the orientation flipping of the morphology. The cyclic transition occurs faster in thick films (177 nm) where the mass uptake and solvent volume fraction is smaller and therefore the driving force for phase separation is higher. We induced a stronger segregation by confining the chains in graphoepitaxially patterned substrates. As expected, the cyclic transition occurred at higher rate. Our work is another step forward to understanding the structure evolution and also controlling the alignment of block copolymer nanocylinders independently of thickness and external fields.

KEYWORDS: nanopattern evolution · block copolymer thin films · cyclical morphology transition · *in-situ* light scattering · graphoepitaxial alignment

Self-organized block copolymer (BCP) systems have been shown to have a host of applications[1,2] most notably in the fabrication of inorganic structures used in electronic, optoelectronic,[3,4] and magnetic devices.[5] Absolute and precise control of pattern orientation (*i.e.*, to the surface plane) is central to their possible use and requires a profound understanding of phase behavior[6] and structure evolution[2,7,8] during postannealing of the BCP films. In this work we demonstrate that pattern orientation coupled to pattern alignment can be achieved for cylinder forming poly(styrene-*b*-ethylene oxide) (PS-*b*-PEO) films. We also show highly unexpectedly cyclic transitions with anneal time of the polymer structure between perpendicular and parallel arrangements of microphase separated cylinders in these films using *in situ* time-resolved light scattering data combined with *ex-situ* time evolution AFM experiments. This is the first time such observations have been reported. In particular, our work shows how orientation of the pattern can be determined independently of the initial film thickness, surface segregation effects, and "solvent fields".[9−14]

Microphase separation in BCP systems has emerged as potentially the most practical self-assembly technique for fabrication of ultrasmall nanoelectronic circuitry. However, achieving long-range ordered patterns of controlled orientation (to surface) and alignment (to an in-plane surface direction) is the key to the industrial development of this technology. To perfect pattern formation for application, a good understanding of structure formation is needed. Thermal annealing and solvent annealing of thin film block copolymers afford a means to sponsor the ordered microphase separation of these systems and so deliver organized patterns for industrial applications.[15] Russell and co-workers have pioneered the use of solvent annealing to direct the orientation of cylindrical patterns at the substrate surface using the "solvent field" generated by solvent evaporation.[16−18] This work, however, demonstrates that solvent annealing is a (poorly understood) dynamic process that may offer considerable advantages in terms of structural control. To this effect, the dynamics of pattern formation in thin films (30 and 177 nm) of cylinder forming PS-*b*-PEO exposed to toluene vapor are detailed herein.

RESULTS AND DISCUSSION

Cyclic Transition. Evidence for structural orientation control and the highly unusual cyclical "flipping" of orientation is shown in Figure 1. These films were solvent annealed at 50 °C with a nominal saturated vapor pressure of toluene about 12.3 kPa. Although these effects occur over a range of temperatures, 50 °C was the optimum temperature to work with as significantly higher temperatures led to severe dewetting of the films and lower temperatures did not provide

* Address correspondence to p.mokarian@ucc.ie.

Received for review January 28, 2011 and accepted May 26, 2011.

Published online May 26, 2011
10.1021/nn2003629

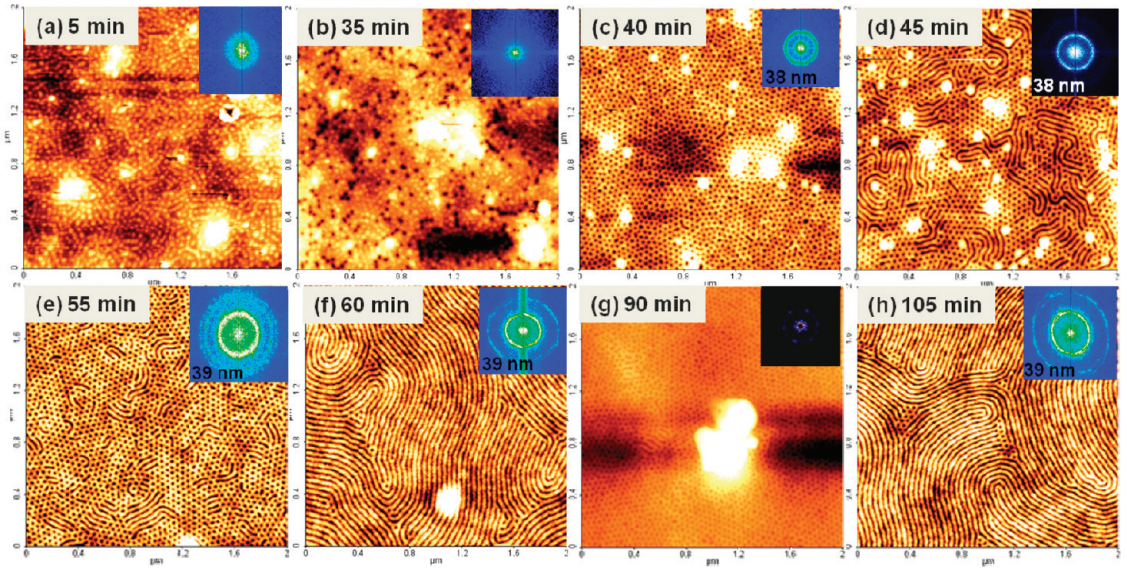

Figure 1. AFM topographic images showing repeated conversion of vertical and parallel orientation in a hexagonal forming PS-*b*-PEO film of 30 nm thick (a) after 5 min exposure to toluene at 12.3 kPa, (b) 35 min, (c) 40 min, (perpendicular arrangement), (d) mixed perpendicular and parallel arrangements, (e) 55 min, (f) 60 min, (g) 90 min, (h) 105 min. The images are 2 × 2 μm^2. The insets are FFT results, showing the pitch of about 39 nm (see text for further details).

sufficient driving force for this transition to occur. AFM images were collected after removal from the vapor. The process of microphase separation appears to begin through the formation of micelle structures (Figure 1a). This configuration is stable for approximately 35 min when small voids begin to appear presumably due to micelle coalescence (Figure 1b). This period appears to represent solvent diffusion through the film. PS is a glassy polymer and in appropriate organic solvent, case II diffusion takes place.[19,20] This is a relatively slow process as the volume fraction of the solvent has to reach a critical value before the polymer chains can extend and relax. At this time a front forms and propagates in the film. After 40 min of exposure the chains are stretched enough for front propagation, mass uptake is large enough, and the phase transition to a vertical cylindrical (*i.e.,* PEO cylinders within a PS matrix) occurs (Figure 1c). Surprisingly, this structure is not the thermodynamically stable state of the final film structure. Once formed, it can be repeatedly transformed between a parallel and vertical orientation depending on solvent anneal time. This is highly unusual as additional solvent exposure normally only refines the structure through defect annihilation. Figure 1 panels d−h represent the recycling of these cylindrical structures. It should be noted that the structures formed extend through the film and are not surface effects only. This can be proven by selective wet/dry etching which removes the PEO cylinders from the outermost surface to the substrate−polymer interface (see Supporting Information, Figures 1−3).

We suggest that this flipping process results directly from a solvent swelling and deswelling process as the number of times this recycling occurs cannot be a result of continued uptake of solvent since the film cannot swell infinitely. As the solvent swells the film, the film reaches a critical thickness where a parallel arrangement is more thermodynamically favorable[9,21] and the film reconstructs to that shown in Figure 1 panels f and h (note that Figure 1d represents an intermediate structure where both vertical and parallel arrangements are observed). It is suggested that the parallel cylinder orientation continuously recycles into the vertical arrangement because this structure cannot maintain the volume of solvent absorbed and effectively "thins" as excess solvent is released. This is schematically illustrated in Figure 2. The release of solvent might be associated with the surface energy differences of the film (surface composition is very different) or because of internal strain differences between the vertical and parallel arrangements. It is clear that for this process to occur, both the vertical and parallel morphologies must have very similar free energies of formation and small differences in conditions allow one structure to realize a different arrangement depending on, for example, thickness of the swelling film, solvent content, *etc.* It should be noted that a recent GISAXS study of structure rearrangement[22] suggests lamellae PS-b-PB (polystyrene-*b*-polybutadiene) systems can go through deswelling within a few minutes after exposure to toluene. However, this is solvent dependent as deswelling in chloroform does not appear to occur for similar films.[23]

Thickness Effect. This phenomenon was observed for all films prepared here and, for example, the cyclical

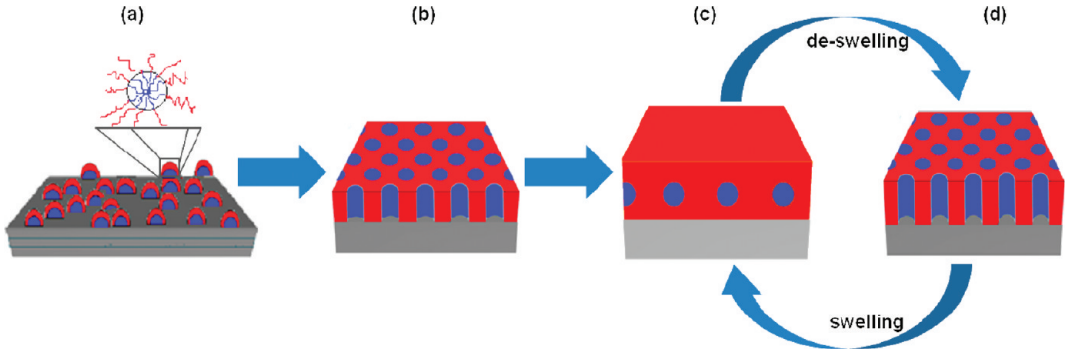

Figure 2. Schematic illustration of structural recycling in PS-*b*-PEO film: (a) micelle formation after exposure to toluene, (b) perpendicular arrangement of the structure due to solvent uptake, (c) parallel orientation due to further swelling, (d) deswelling leads to flipping of the parallel to vertical alignment.

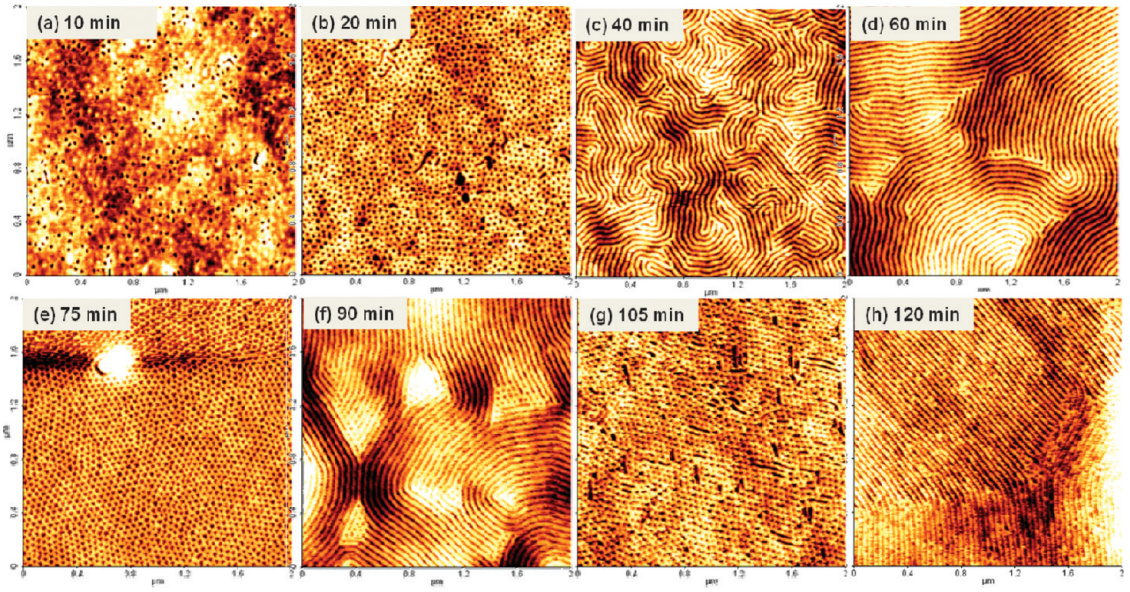

Figure 3. Cyclic transition in thick (177 nm) PS-*b*-PEO films exposed to toluene for different annealing times. A transformation similar to thin film (shown in Figure 1) happens but at higher transition rate. A parallel structure is formed after 40 min (c) as opposed to 60 min in Figure (1c). The images are 2 × 2 μm^2.

nature of structural evolution was not affected by the initial film thickness. A thick film (177 nm) shows a similar behavior to the thinner film but the rate of structural conversion is significantly quicker in the thicker film. In Figure 3b, after 20 min the perpendicular cylinders are already formed. For the thinner film it takes 40 min to reach this point (see Figure 3c). This is followed by a parallel orientation of cylinders (Figure 3c) which grow in length through the annealing process (see Figure 3c,d,f,h). The more rapid transition in thick films could be due to lower solvent uptake. By increasing the film thickness, the mass uptake and, therefore, the solvent volume fraction in the film decrease,[23] leading to a strong Flory–Huggins interaction parameter between the polymer segments which induces the driving force for the early phase separation (see eq 1).

$$\chi_{\text{eff}} = \chi(1 - \varphi_s) \qquad (1)$$

where χ_{eff} and χ are the Flory–Huggins interaction parameters in the presence and absence of the solvent. φ_s is the volume fraction of solvent.

***In Situ* Time-Resolved Light Scattering.** To validate the tentative model described here, we have performed an *in situ* time-resolved light scattering experiment in an environmental cell allowing samples to be annealed under different toluene pressures. This allowed the verification of the case II diffusion scenario (through the threshold value for vapor pressure) and monitoring of the solvent uptake through reflectivity. The vapor pressure in the reaction chamber was established by flowing nitrogen through a temperature controlled solvent reservoir so that the solvent vapor pressure was determined by the reservoir temperature. Figure 4 is the schematic diagram of the setup. To perform the experiment at 50 °C and to avoid condensation, most of the experimental set up parts including the bubbler, all tubes carrying the gas, and the environmental

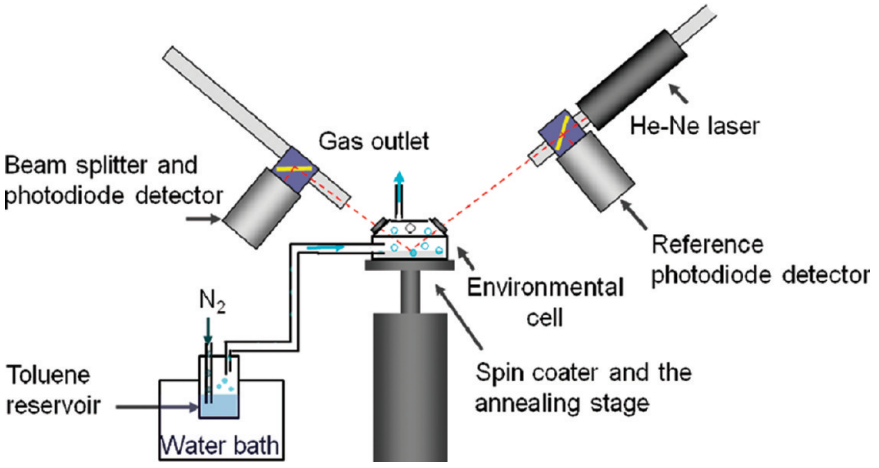

Figure 4. Schematic diagram showing the main components of the *in situ* light scattering set up during solvent and thermal annealing in a custom made environmental cell.[24] Nitrogen was blown into a toluene reservoir. The temperature of the reservoir was controlled in a water bath. The cell can be saturated with toluene with different nominal vapor pressures. The reflectivity–time data was recorded during the annealing. To avoid wall condensations, most components were wrapped in heating tapes (not shown here).

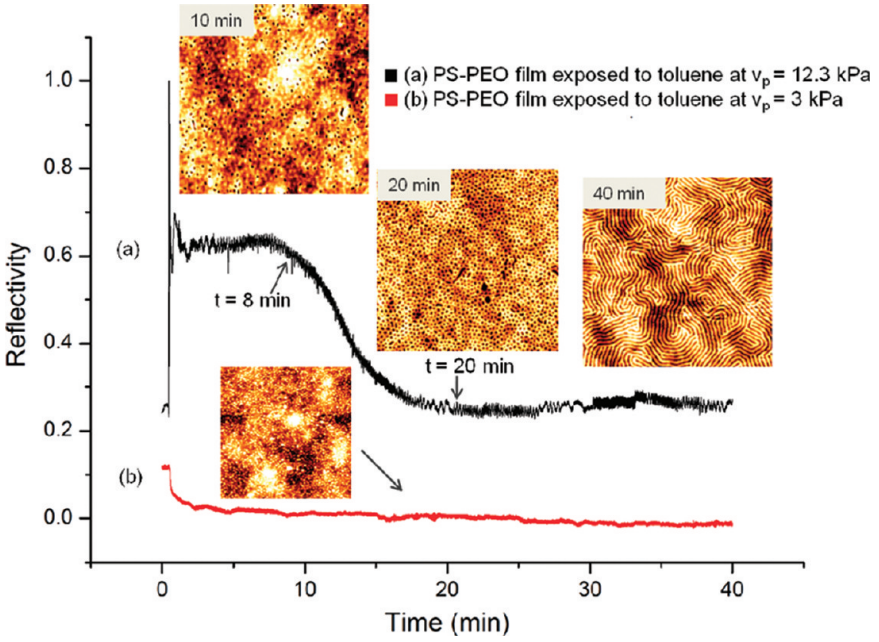

Figure 5. Specular reflectivity measured during the exposure of the PS-*b*-PEO film to toluene vapor (a) at 12.3 kPa and (b) 3 kPa. The insets are AFM images during structure evolution. At high vapor pressure there are three different regimes correspond to different morphologies formed during that time. At low vapor pressure there is no change in reflectivity during the exposure and also no morphology evolution, suggesting a vapor pressure threshold is needed for the transition. The insets AFM images are 2 × 2 μm^2.

chamber were wrapped in heating tapes (not shown here). The temperature was set 1 °C above the annealing temperature at 51 °C to avoid condensation and was controlled by thermometers at different points. More details about this experimental set up can be found elsewhere.[24] Figure 5 shows reflectivity–time graphs during toluene exposure of PS-*b*-PEO film at saturated vapor pressures of 12.3 kPa (50 °C) and 3 kPa (at 12 °C). In both cases there is an immediate change in reflectivity after exposure to toluene. According to the Fresnel equation, reflectivity is a function of the thickness. Therefore the change in reflectivity is due to change in thickness and density. However, there is a clear difference between the reflectivity changes and the structure evolution at low and high vapor pressure (Figure 5). When the film is exposed to toluene at low vapor pressure (3 kPa), there is no structural change after 120 min (see the insets Figure 5b). This is because micelles form within 5 min of exposure and remain stable (see the lower inset in Figure 5). Also after the initial drop in reflectivity which is due to swelling and an increase in film

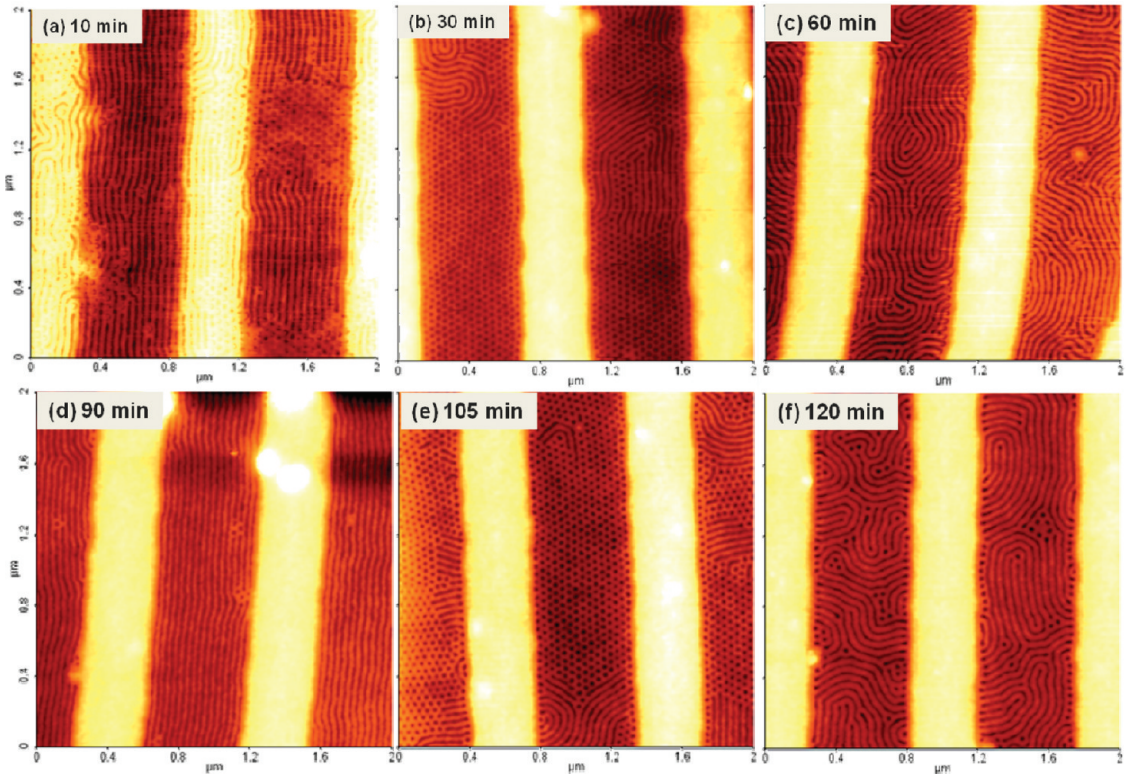

Figure 6. The effect of graphoepitaxy on cyclic transition. (a) The parallel lines form quickly, within 10 min of exposure. Then the structure fluctuates between dotes and lines (b and c). It reaches the best parallel alignment after 90 min. (e and f) More transition of perpendicular and parallel rays of cylinder. The images are 2 × 2 μm^2.

thickness, there are no further pronounced changes (Figure 5b). It is thought that at lower vapor pressure (3 kPa), the osmotic pressure that acts on a semipermeable surface of a glassy polymer is not high enough to overcome the resistance exerted by immobilized chains in glassy PS. A contact angle measurement ($\alpha = 74°$) at a similar surface is consistent with the top layer consisting of hydrophobic glassy PS. At high vapor pressure (12 kPa) there are three different regimes in Figure 5a. After an immediate change in the reflectivity due to a change in refractive index, a metastable equilibrium state is achieved for about 8 min. The small fringes are due to interference effects of the laser light from the top of the film and the polymer–substrate interface. After about 8–10 min there is a sharp but gradual decrease in the reflectivity before it plateaus. Between 30 and 40 min there is a discernible (but relatively small) increase in the reflectivity. The changes in the reflectivity observed are consistent with the AFM time evolution experiment shown in Figure 3. Three distinct reflectivity regimes in Figure 5 correspond to the formation of the initial three different patterns formed in PS-*b*-PEO films, as shown in the AFM images in Figure 3. The interval of 0–8 min represents the micelle structure, 8–25 min represents vertical cylinder formation and stability while 25–35 min represent horizontal cylinder structure formation. The effect of the temperature is controversial in our experiment. While the higher temperature is expected to decrease the Flory–Huggins interaction parameter and therefore reduce the driving force for separation, in our experiment the phase separation and the subsequent cyclic transition happens at higher temperature. One possible reason could be due to accessibility of the polymer chains to the solvent in interior film. Low temperature does not provide enough pressure for the solvent to diffuse into the glassy layer easily. This can be clearly seen in Figure 5b in which the change in reflectivity (which reflects the change in thickness) is not apparent. On the other hand in Figure 5a, the high temperature provides enough vapor pressure for diffusion of the vapor in the film and creates enough chain mobility for structure configuration. However, because of the complicated relationship of the reflectivity with thickness, it is not easy to predict the exact trend of thickness change during the swelling. But nevertheless, three distinctive regimes in reflectivity–time data (Figure 5a) and the coincidence of time duration of each zone with structural change in AFM images back up our theory that the structural changes are related to thickness fluctuations.

Graphoepitaxy. If solvent exposure is to be a practical (*e.g.*, to define parallel nanowire structures) method of controlling nanopattern orientation, it is also necessary

to combine the solvent anneal methodology with a technique such as graphoepitaxy[5,25−28] that facilitates pattern alignment (i.e., relative to an in-plane surface direction). These methods of directing the self-assembly process may impose additional boundary conditions which may prevent orientation control. Therefore, substrates were studied that were engineered with parallel channels of 400 nm width and 30 nm depth. Samples were prepared and processed similar to the methodology described in Figure 1. The film thickness was sufficient to just fill the channels, that is, about 30 nm (just enough to allow parallel cylinder morphologies), and the films demonstrated that orientation control coupled to directed alignment of both vertical and parallel pattern orientations could be achieved (Figure 6). Ordered pattern formation is very rapid (indeed little evidence of micelle formation was observed even prior to solvent annealing) and the first ordered phase observed is a parallel arrangement of cylinders. As can be seen in Figure 6, the morphology of the cylinder structure switches between parallel and perpendicular arrangements with time, but at a significantly faster rate than seen on flat substrates. The films also exhibit strong graphoepitaxial effects typical of the PS-*b*-PEO system,[29] because PEO interacts strongly with a silica surface because of its higher polarity compared to that of PS.[30] This could account for the faster kinetics as graphoepitaxy is mediated by the strong interaction of one component with the topography and so induces component segregation.[31] In strongly segregated block copolymers, the chains are more stretched and solvent uptake happens faster,[23] thus explaining the faster kinetics for both microphase separation and structure cycling.

CONCLUSIONS

In summary, we have demonstrated continuous control of pattern structure and alignment through solvent exposure. We have investigated the nature of a cyclic transition observed in PS-*b*-PEO thin films during the solvent annealing process. The morphology fluctuates between perpendicular and parallel arrays of cylinders over time. *In-situ* light scattering measurements during solvent annealing are consistent with a model where structure cycles according to amount of solvent in the film. The data indicate that there is a threshold value (∼12 kPa at 50 °C) for the vapor pressure and solvent volume fraction in the film necessary for the full structural transitions to occur. This can be related to a case II diffusion in which a critical value of solvent is needed for formation and propagation of the front through the film. The cyclic structural transitions occur faster in both thick and topographically confined films consistent with a mechanism where structural transitions are related to solvent volume uptake.

METHODS

Materials. We used polystyrene-*block*-polyethylene oxide (PS-*b*-PEO) block copolymer purchased from Polymer Source with average molecular masses of blocks M_{PS} = 42 kg mol^{-1} and M_{PEO} = 11.5 kg mol^{-1} and polydispersity of 1.07. Thin and thick (30 and 177 nm) PS-*b*-PEO films were spun cast from HPLC toluene solution from Sigma-Aldrich onto bare and topographically patterned silicon substrates with 2 nm thick native oxide layer. The silicon substrates were provided and patterned by Intel using electron beam lithography techniques.

Characterization. For solvent annealing, the films were placed inside individual screw cap bottles of 100 mL volume with a toluene reservoir and were placed in the oven. The saturated vapor pressure of a gas is a function of temperature only, which means that by changing the temperature we are able to change the vapor pressure of the gas inside the cell. The films were exposed to toluene at different nominal vapor pressures, 12.3 kPa (at 50 °C) and 3 kPa (at 12 °C) for different periods of time. Every 5−10 min one sample was removed from the oven. The samples were quenched at room temperature. The topographic and phase images of the films were recorded with a Park XE-100 AFM system in noncontact mode with a silicon microcantilever probe tip with a force constant of 60000 N m^{-1} to study the structure evolution. Film thickness was measured by Woollam spectroscopic ellipsometer M-2000U.

In situ time-resolved light scattering experiments were performed in a custom-made environmental cell (Figure 4) that was heated by heating tapes to prevent wall condensation. During the annealing, a laser beam (He−Ne, 633 nm) incident on the sample is reflected. The intensity of the incident and the reflected light is measured by two photodiodes. The specular reflection (reflectivity) was collected for 40 min and the reflectivity−time data were analyzed.

Acknowledgment. We gratefully acknowledge the SFI CSET CRANN grant for funding this project. We would like to thank University of Sheffield for access to the *in situ* light scattering experimental setup. We appreciate the assistance provided by the staff of AML (Advanced Microscopy Laboratory) in CRANN. The authors thank Intel for providing us with the patterned substrates through the adaptive grid substrate programme.

Supporting Information Available: AFM image of as-cast PS-*b*-PEO film, SEM, and TEM cross section of PS-PEO patterns. This material is available free of charge *via* the Internet at http://pubs.acs.org.

REFERENCES AND NOTES

1. Hamley, I. W. Ordering in Thin Films of Block Copolymers: Fundamentals to Potential Applications. *Prog. Polym. Sci.* **2009**, *34*, 1161–1210.
2. Tsarkova, L.; Sevink, G. J. A.; Krausch, G., Nanopattern Evolution in Block Copolymer Films: Experiment, Simulations and Challenges. In *Complex Macromolecular Systems I*; Springer-Verlag Berlin: Berlin, 2010; Vol. 227, pp 33−73.
3. Qiang, L. L.; Ma, Z.; Zheng, Z.; Yin, R.; Huang, W. Novel Photo-Crosslinkable Light-Emitting Rod/Coil Copolymers: Underlying Facile Material for Fabricating Pixelated Displays. *Macromol. Rapid Commun.* **2006**, *27*, 1779–1786.
4. Darling, S. B. Block Copolymers for Photovoltaics. *Energy Environ. Sci.* **2009**, *2*, 1266–1273.
5. Xiao, S. G.; Yang, X. M.; Edwards, E. W.; La, Y. H.; Nealey, P. F. Graphoepitaxy of Cylinder-Forming Block Copolymers for Use as Templates To Pattern Magnetic Metal Dot Arrays. *Nanotechnology* **2005**, *16*, S324–S329.
6. Knoll, A.; Horvat, A.; Lyakhova, K. S.; Krausch, G.; Sevink, G. J. A.; Zvelindovsky, A. V.; Magerle, R. Phase Behavior in

Thin Films of Cylinder-Forming Block Copolymers. *Phys. Rev. Lett.* **2002**, *89*, 4.
7. Knoll, A.; Lyakhova, K. S.; Horvat, A.; Krausch, G.; Sevink, G. J. A.; Zvelindovsky, A. V.; Magerle, R. Direct Imaging and Mesoscale Modelling of Phase Transitions in a Nanostructured Fluid. *Nat. Mater.* **2004**, *3*, 886–890.
8. Wang, Y.; Hong, X. D.; Liu, B. Q.; Ma, C. Y.; Zhang, C. F. Two-Dimensional Ordering in Block Copolymer Monolayer Thin Films Upon Selective Solvent Annealing. *Macromolecules* **2008**, *41*, 5799–5808.
9. Knoll, A.; Magerle, R.; Krausch, G. Phase Behavior in Thin Films of Cylinder-Forming ABA Block Copolymers: Experiments. *J. Chem. Phys.* **2004**, *120*, 1105–1116.
10. Anastasiadis, S. H.; Russell, T. P.; Satija, S. K.; Majkrzak, C. F. Neutron Reflectivity Studies of the Surface-Induced Ordering of Diblock Copolymer Films. *Phys. Rev. Lett.* **1989**, *62*, 1852–1855.
11. Matsen, M. W. Self-Assembly of Block Copolymers in Thin Films. *Curr. Opin. Colloid Interface Sci.* **1998**, *3*, 40–47.
12. Hamley, I. W. Nanostructure Fabrication Using Block Copolymers. *Nanotechnology* **2003**, *14*, R39–R54.
13. Fasolka, M. J.; Mayes, A. M. Block Copolymer Thin Films: Physics and Applications. *Annu. Rev. Mater. Res.* **2001**, *31*, 323–355.
14. Jones, R. A. L.; Norton, L. J.; Kramer, E. J.; Bates, F. S.; Wiltzius, P. Surface-Directed Spinodal Decomposition. *Phys. Rev. Lett.* **1991**, *66*, 1326–1329.
15. O'Driscoll, S. M.; O'Mahony, C. T.; Farrell, R. A.; Fitzgerald, T. G.; Holmes, J. D.; Morris, M. A. Toroid Formation in Polystyrene-*block*-poly(4-vinyl pyridine) Diblock Copolymers: Combined Substrate and Solvent Control. *Chem. Phys. Lett.* **2009**, *476*, 65–68.
16. Kim, S. H.; Misner, M. J.; Xu, T.; Kimura, M.; Russell, T. P. Highly Oriented and Ordered Arrays from Block Copolymers *via* Solvent Evaporation. *Adv. Mater.* **2004**, *16*, 226–231.
17. Elbs, H.; Drummer, C.; Abetz, V.; Krausch, G. Thin Film Morphologies of ABC Triblock Copolymers Prepared From Solution. *Macromolecules* **2002**, *35*, 5570–5577.
18. Fukunaga, K.; Elbs, H.; Magerle, R.; Krausch, G. Large-Scale Alignment of ABC Block Copolymer Microdomains *via* Solvent Vapor Treatment. *Macromolecules* **2000**, *33*, 947–953.
19. Alfrey, T.; Gurnee, E. F.; Lloyd, W. G. Diffusion in Glassy Polymers. *J. Polym. Sci., Part C: Polym. Symp.* **1966**, *12PC*, 249–261.
20. Thomas, N. L.; Windle, A. H. A Theory of Case-II Diffusion. *Polymer* **1982**, *23*, 529–542.
21. Horvat, A.; Lyakhova, K. S.; Sevink, G. J. A.; Zvelindovsky, A. V.; Magerle, R. Phase Behavior in Thin Films of Cylinder-Forming ABA Block Copolymers: Mesoscale Modeling. *J. Chem. Phys.* **2004**, *120*, 1117–1126.
22. Papadakis, C. M.; Di, Z. Y.; Posselt, D.; Smilgies, D. M. Structural Instabilities in Lamellar Diblock Copolymer Thin Films during Solvent Vapor Uptake. *Langmuir* **2008**, *24*, 13815–13818.
23. Zettl, U.; Knoll, A.; Tsarkova, L. Effect of Confinement on the Mesoscale and Macroscopic Swelling of Thin Block Copolymer Films. *Langmuir* **2010**, *26*, 6610–6617.
24. Mokarian-Tabari, P.; Geoghegan, M.; Howse, J. R.; Heriot, S. Y.; Thompson, R. L.; Jones, R. A. L. Quantitative Evaluation of Evaporation Rate during Spin Coating of Polymer Blend Films: Control of Film Structure Through Defined-Atmosphere Solvent Casting. *Eur. Phys. J. E: Soft Matter Biol. Phys.* **2010**, *33*, 283–289.
25. Kim, S. O.; Solak, H. H.; Stoykovich, M. P.; Ferrier, N. J.; de Pablo, J. J.; Nealey, P. F. Epitaxial Self-Assembly of Block Copolymers on Lithographically Defined Nanopatterned Substrates. *Nature* **2003**, *424*, 411–414.
26. Segalman, R. A.; Yokoyama, H.; Kramer, E. J. Graphoepitaxy of Spherical Domain Block Copolymer Films. *Adv. Mater.* **2001**, *13*, 1152–1155.
27. Cheng, J. Y.; Zhang, F.; Smith, H. I.; Vancso, G. J.; Ross, C. A. Pattern Registration Between Spherical Block-Copolymer Domains and Topographical Templates. *Adv. Mater.* **2006**, *18*, 597–601.
28. Sundrani, D.; Darling, S. B.; Sibener, S. J. Guiding Polymers to Perfection: Macroscopic Alignment of Nanoscale Domains. *Nano Lett.* **2004**, *4*, 273–276.
29. Thomas G. Fitzgerald, R. A. F.; O'Driscoll, Sheena; O'Mahony, Colm T.; Holmes, Justin D.; Morris, Michael A. Orientation and Translational Control of PS-*b*-PEO/PS Thin Films *via* Solvent Annealing and Graphoepitaxy Techniques. *e-J. Surf. Sci. Nanotechnol.* **2009**, *7*, 471–475.
30. Neto, C.; James, M.; Telford, A. M. On the Composition of the Top Layer of Microphase Separated Thin PS-PEO Films. *Macromolecules* **2009**, *42*, 4801–4808.
31. Farrell, R. A.; Fitzgerald, T. G.; Borah, D.; Holmes, J. D.; Morris, M. A. Chemical Interactions and Their Role in the Microphase Separation of Block Copolymer Thin Films. *Int. J. Mol. Sci.* **2009**, *10*, 3671–3712.